analytical chemistry

pubs.acs.org/ac Article

Label-Free and Ultrasensitive Detection of Butyrylcholinesterase and Organophosphorus Pesticides by Mn(II)-Based Electron Spin Resonance Spectroscopy with a Zero Background Signal

Li Tang, Chunyu Wang, Sizhu Tian, Zhimin Zhang, Yong Yu, Daqian Song, and Ziwei Zhang*

Cite This: *Anal. Chem.* 2022, 94, 16189−16195 Read Online

ACCESS | Metrics & More | Article Recommendations | Supporting Information

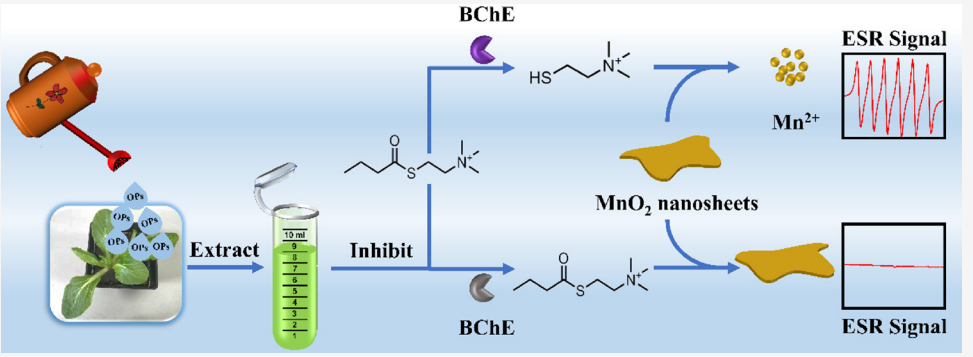

ABSTRACT: Mn(II)-based electron spin resonance (ESR) spectroscopy was used for detecting butyrylcholinesterase (BChE) and organophosphorus pesticides (OPs). MnO_2 nanosheets were synthesized with manganese chloride and hydrogen peroxide. With the catalysis of BChE, S-butyrylthiocholine iodide (BTCh) was hydrolyzed into thiocholine which has a reducing −SH group. In the presence of thiocholine, MnO_2 nanosheets were broken down and Mn(IV) in MnO_2 nanosheets was reduced into Mn(II). Mn^{2+} is a paramagnetic ion and gives a good ESR signal. In contrast, MnO_2 nanosheets have no ESR signal and need not be separated from Mn^{2+}. Mn^{2+} can be determined directly by ESR spectroscopy, and no further sensing probe is needed. ESR spectroscopy based on directly detecting Mn^{2+} is much simpler than those using other probes besides MnO_2. The ESR signal of Mn^{2+} is proportional to the catalytic activity of BChE. OPs which inhibit the activity of BChE can also be detected by probing the ESR signal of Mn^{2+}. Since there is no ESR signal of MnO_2 nanosheets, the background signal in the absence of BChE was close to zero. The limit of detection (LOD) of BChE was as low as 0.042 U L^{-1}. The standard curve for determining the OP paraoxon was established by measuring the inhibition of BChE by paraoxon, and the LOD of paraoxon was found to be 0.076 ng mL^{-1}. The spiked Chinese cabbage extract samples were analyzed, and the experimental results indicated that the recoveries were from 96.5 to 102.8%. The planted Chinese cabbage was sprayed with the paraoxon solution, and the residue amount of paraoxon in the extract was estimated by the method. The result obtained by the present method was consistent with that obtained by HPLC, which proved the practicability of this new method.

INTRODUCTION

Butyrylcholinesterase (BChE) is a nonspecific cholinesterase that can hydrolyze a variety of choline esters. It is an essential indicator for the prediction and diagnosis of many diseases, including liver damage, Alzheimer's disease, and organophosphorus pesticide (OP) poisoning.[1] Therefore, accurate determination of BChE's activity has practical significance. So far, colorimetric and fluorescence methods were most commonly used in the evaluation of BChE's activity.[2] Nevertheless, when the colorimetric assay was applied, other substances in the sample easily interfered with the determination of analytes and the sensitivity was found to be low; when the fluorescence method was applied, the sensitivity was found to be high, but toxic materials such as quantum dots were used in many cases.

OPs are extensively used in agriculture in order to control or eliminate pests because of their high efficiency, low bioaccumulation, and rapid biodegradation.[3] However, due to the abuse of OPs, pesticide residues and their metabolites in water resources, fruits, and vegetables are harmful to human

Received: August 24, 2022
Accepted: October 26, 2022
Published: November 4, 2022

health.[4] Meanwhile, OPs inhibit the activity of cholinesterase by combining with cholinesterase, resulting in a series of neurological diseases and even death.[5] Considering the toxicity of OPs and their residues, it is necessary to establish a fast and straightforward quantification strategy for OPs in food and environment samples. To date, the methods for detecting OPs mainly include mass spectrometry,[6,7] gas chromatography/mass spectrometry (GC/MS),[8,9] liquid chromatography,[10] immunoassay,[11] surface-enhanced Raman spectroscopy,[12] electrochemistry,[13] and fluorescence spectroscopy.[14] However, these methods still have disadvantages such as complicated sample preparation or a time-consuming measurement. As compared with these methods, a simpler and rapider sensing method is needed and presented in this study.

MnO_2 nanosheets have received extensive attention due to their excellent physical and chemical properties.[15] MnO_2 nanosheets can be decomposed and reduced to Mn^{2+} by reductive substances. This reaction has been utilized by many researchers in detecting GSH or enzymes which catalyze the generation of reductive products.[3,16] So far, in most studies, neither MnO_2 nor Mn^{2+} is directly monitored. An extra sensing probe such as a fluorescent nanoparticle, an electrochemiluminescence reagent, or a Raman probe is introduced.[3,17,18] For example, Yan et al. synthesized fluorescent carbon dots, and the fluorescence was quenched by MnO_2 nanosheets and recovered when MnO_2 nanosheets were decomposed by the reductive hydrolysate of BChE.[3] In few publications, Mn^{2+} was directly monitored by inductively coupled plasma-mass spectrometry (ICP-MS).[19] However, Mn^{2+} had to be separated from MnO_2 before quantification by ICP-MS. Benefiting from the unique capability of ESR spectroscopy in direct and sensitive detection of Mn^{2+}, this research provides a novel label-free method with no need of synthesizing an extra probe. Also, the zero signal of MnO_2 nanosheets on the ESR spectrometer saves the procedure of separating MnO_2 from Mn^{2+} as well as guarantees a close-to-zero background.

Electron spin resonance (ESR), also called electron paramagnetic resonance (EPR), mainly studies the spin levels under the action of an external magnetic field. The research objects of ESR spectroscopy include free radicals, transition/rare-earth metal ions and their compounds, as well as impurities and defects in solids.[20] Since the ESR technique has some unique and excellent performances, such as high measurement sensitivity, a small amount of sample required, and no damage to the detection sample,[21,22] it has been widely applied in many fields such as food science, biology, physics, chemistry, and medicine.[23]

Herein, we developed a method to quantitatively detect BChE and OPs in plant samples based on directly measuring Mn^{2+} by ESR spectroscopy. In this strategy, MnO_2 nanosheets with no ESR signal are reduced into Mn^{2+} by thiocholine generated from the reaction catalyzed by BChE. Mn^{2+} can be detected by ESR spectroscopy, thus the ESR signal is "turned on". OPs can inhibit the activity of BChE, resulting in less cracking of MnO_2 nanosheets, less yield of Mn^{2+}, and finally a decrease in ESR signal. Paraoxon as an OP was used to test the method, and the paraoxon residue in Chinese cabbage was further examined.

EXPERIMENTAL SECTION

Reagents. BChE from equine serum (the activity of BChE is 7.51 units/mg; unit definition: 1 unit hydrolyzes ≥1mole of acetylcholine per minute at 25 °C, pH 7.4) and S-butyrylthiocholine iodide (BTCh) were purchased from Aladdin Industrial Corporation, Shanghai, China. Paraoxon was purchased from Beijing Manhage Biotechnology Company. Paraoxon was purchased as the standard solution dissolved in acetone, and the purity was 99.8%. The information for other OPs and the reagents used in the experiments are placed in the Supporting Information.

Determination of BChE's Activity. 100 μL of various concentrations of BChE was added into the mixed solution containing 100 μL of BTCh and 100 μL of 10 mmol L^{-1} 4-(2-hydroxyethyl)-1-piperazineethanesulfonic acid (HEPES) at pH 8.0. The resulting solution was incubated at 37 °C for 60 min and then mixed with 100 μL of MnO_2 nanosheets. The concentrations of BTCh and MnO_2 nanosheets in the resulting solution were, respectively, 1.25 mmol L^{-1} and 0.25 mg mL^{-1}. The mixture reacted at room temperature for 50 min, resulting in the analytical sample. Subsequently, the ESR spectrum was collected for the analytical sample.

Detection of OPs. For OPs' detection, paraoxon was selected to establish a standard curve. Before use, the purchased paraoxon standard solution was diluted to the desired concentration with water. 50 μL of different concentrations of paraoxon was incubated with 50 μL of BChE for 30 min and then reacted with the mixture of BTCh and HEPES. After an incubation of 60 min at 37 °C, the solution was mixed with MnO_2 nanosheets for a reaction of 50 min at room temperature. The resulting solution was referred to as an analytical sample and ready for the ESR measurement.

Analysis of the Analytical Sample by ESR. The analytical sample (15 μL) was transferred using a pipettor into a glass capillary tube with an inner diameter of 0.8 mm. The glass capillary tube was then inserted into the quartz tube with a diameter of 4 mm. The quartz tube was put into the resonator cavity of the X-band E500 ESR spectrometer. The spectrum was recorded at room temperature. For each data point, three parallel experiments were performed. In order to improve the repeatability of parallel experiments, the quartz tube was kept constant in the resonator cavity, and only the sample tube was replaced when switching to the next sample.

The instrumental setting of the ESR spectrometer is listed below: the magnetic field range for the spectrum was from 3020 to 3690 Gauss; each spectrum had 1024 data points; the microwave frequency was about 9.41 GHz; the modulation amplitude was 8.0 Gauss; the microwave power was 20 mW; the time constant was 164 ms; the conversion time was 160 ms.

Detection of Paraoxon in the Chinese Cabbage Extract. Two groups of Chinese cabbage were cultivated under the same conditions. One group of Chinese cabbage was sprayed with 25 mL of 0.6 μg mL^{-1} paraoxon solution once every other day for 3 times. The other group was not sprayed with the paraoxon solution and cultivated as the control group. The day after the last spray, 4 g of Chinese cabbage was collected and mashed. 4 mL of methanol was added so as to extract the paraoxon. The resulting solution was ultrasonicated for 30 min and centrifuged for 10 min at 6000 rpm. After that, the solution was filtered through a 0.22 μm pore size membrane filter and used as the extract of sprayed Chinese cabbage.

RESULTS AND DISCUSSION

Characterization of MnO_2 Nanosheets. Bulk MnO_2 was synthesized based on a redox reaction between manganese

https://doi.org/10.1021/acs.analchem.2c03708
Anal. Chem. 2022, 94, 16189−16195

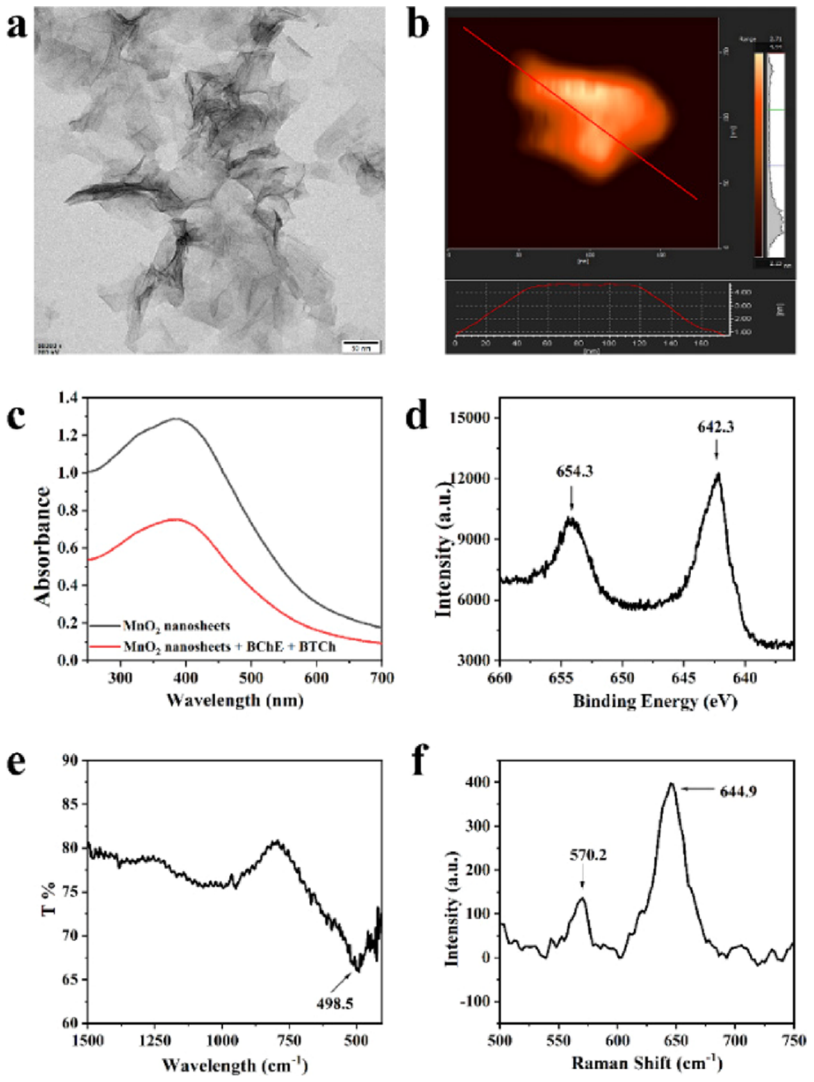

Figure 1. (a) TEM image of MnO_2 nanosheets; (b) AFM image of MnO_2 nanosheets; (c) UV−vis spectra of MnO_2 nanosheets in the absence (black line) and in the presence of BChE and BTCh (red line); (d) XPS spectrum of MnO_2 nanosheets; (e) FT-IR spectra of MnO_2 nanosheets; (f) Raman spectra of MnO_2 nanosheets.

chloride tetrahydrate ($MnCl_2{\cdot}4H_2O$) and H_2O_2 in the presence of tetramethylammonium hydroxide (TMA·OH), in which H_2O_2 acts as the oxidant and $MnCl_2$ acts as the manganese source. MnO_2 nanosheets were obtained by ultrasonically dispersing bulk MnO_2 (Figure S1). The morphology of MnO_2 nanosheets was characterized by TEM. As seen in Figure 1a, MnO_2 nanosheets exhibit a distinct sheet-like morphology. The thickness of MnO_2 nanosheets was 3.5 nm estimated by AFM (Figure 1b). Such a typical 2D structure with occasional folds and wrinkles enables MnO_2 nanosheets to have a large surface area. In the UV−vis absorption spectrum (Figure 1c, black curve), MnO_2 nanosheets present an absorption band in the range of 200−700 nm. When BChE and BTCh were added, the yielded thiocholine caused the destruction of MnO_2 nanosheets, resulting in a decrease in the UV−vis absorption intensity (Figure 1c, red curve). The synthesized MnO_2 nanosheets were also studied by XPS. As seen in Figure 1d, two peaks at 642.3 and 654.3 eV are assigned to Mn 2p3/2 and Mn 2p1/2, respectively. Figure 1e displays the FT-IR spectrum of the sample prepared in KBr pellets, and the peak around 498.5 cm^{-1} can be attributed to the Mn−O bond. The Raman spectrum recorded with a 785 mm diode laser is displayed in Figure 1f, and the Mn−O stretching vibration can be observed at 570.2 and 644.9 cm^{-1}. All these results demonstrate the successful preparation of MnO_2 nanosheets.

Sensing Mechanism. As shown in Figure 2, when the enzyme BChE is not added to the reaction system, the

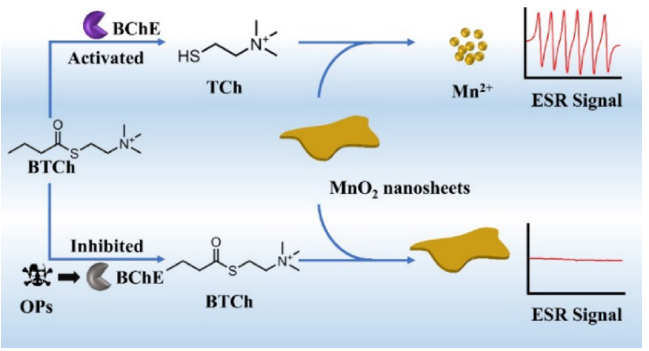

Figure 2. Schematic diagram of the sensing strategy for the detection of OPs by the ESR method.

https://doi.org/10.1021/acs.analchem.2c03708
Anal. Chem. 2022, 94, 16189−16195

substrate BTCh does not react with MnO_2 nanosheets. The MnO_2 nanosheets have no ESR signal at room temperature, and the recorded spectrum was almost a flat horizontal line that is very close to the background signal of the instrument with a blank sample (see Figure 3a at [BChE] = 0 U L^{-1}).

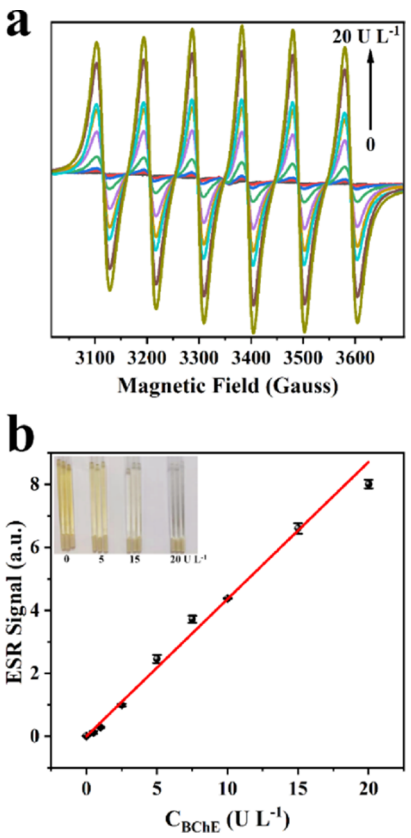

Figure 3. (a) ESR spectra for analytical samples with different concentrations of BChE (0, 0.5, 1.0, 2.5, 5.0, 7.5, 10, 15, 20 U L^{-1}) in the presence of BTCh. (b) Plot of ESR signal vs BChE's concentration and its linear fit. Inset shows the color change of analytical samples in capillary tubes (three analytical samples in capillary tubes for each concentration) with increasing BChE's concentration from 0 to 20 U L^{-1} (i.e., from 0 to 2.66 mg L^{-1}). The error bar represents SD.

However, when the enzyme BChE is added, it catalyzes the hydrolysis of BTCh and produces thiocholine (TCh) which has a reducing −SH group. TCh reduces Mn^{4+} in MnO_2 nanosheets into Mn^{2+}.

Mn^{2+} is paramagnetic with five unpaired electrons. The ESR spectrum of Mn^{2+} in aqueous solution has six almost equally spaced hyperfine lines according to the nuclear spin of Mn^{55} (I = 5/2).[24,25] Thus, the signal of Mn^{2+} can be directly recorded by an ESR spectrometer. The spectra for the analytical samples with different enzyme concentrations displayed in Figure 3a show a typical six-line Mn^{2+} signal in aqueous solution. The distance between two adjacent spectral lines is on average about 95 Gauss. The intensity of the spectrum is proportional to the concentration of produced Mn^{2+} and thus proportional to the concentration of BChE. Since all the spectra have exactly the same lineshape, the peak-to-peak height of the 5th spectral line is used to represent the ESR signal for establishing standard curves.

When OP (e.g., paraoxon) was either sprayed on the plant leaves or spiked into the plant extract, the enzyme activity was inhibited and the amount of produced Mn^{2+} decreased. Therefore, the height of the Mn^{2+} ESR signal is also a good indicator for the existence of trace OP.

Analytical Performances for the BChE Assay. Before systematically studying the sensing performance of the present method to BChE, the concentration of MnO_2, BTCh's concentration, the reaction time, and the pH of the reaction solution were optimized, as shown in Figure S2. A series of ESR spectra for Mn^{2+} at varied BChE concentrations (0, 0.5, 1.0, 2.5, 5.0, 7.5, 10, 15, 20 U L^{-1}) in the presence of 1.25 mmol L^{-1} BTCh are displayed in Figure 3a. Among the six spectral lines of Mn^{2+}, the three lines in the middle (3rd, 4th, and 5th lines) have the smallest linewidth and the highest peak-to-peak amplitude. However, there is a tiny singlet signal from the sample tube that would interfere with the 3rd and 4th lines of Mn^{2+} when the concentration of Mn^{2+} is very low. Thus, the 5th line is picked, and its height is used as the ESR signal when constructing a standard curve. The standard curve (ESR signal vs BChE concentration) is plotted in Figure 3b and simulated using a linear function. The regression equation is ESR signal = 0.43542 (±0.00596) [BChE] + 0.00548 (±0.01816), and a good linear relationship between the ESR signal and BChE concentration was obtained (r = 0.9992). The limit of detection (LOD) of the method (3SD/slope with n = 7) for sensing BChE's activity is estimated to be as low as 0.042 U L^{-1}.

In Table S1, the LOD and detection range of the present method are compared with those from some published methods. The LOD of the present method (0.042 U L^{-1}) is low enough considering that the LODs in publications listed in Table S1 lie between 0.000018 and 79.69 U L^{-1}. The detection range of the present method (0.14−20 U L^{-1}) spreads over more than 2 orders of magnitude. Such a wide detection range is also satisfactory compared with those reported in other works in Table S1, which are between 1 and 2 orders of magnitude.

Interference Studies. To demonstrate the selectivity and anti-interference capability of this method, nine substances commonly existing in plants, including K^+, Na^+, Ca^{2+}, Mg^{2+}, glycine (Gly), alanine (Ala), leucine (Leu), glucose (Glu) at 0.5 mmol L^{-1}, and glucose oxidase (GOx) at 160 U L^{-1}, were added into the catalytic reaction system individually. Figure S3 shows that the ESR signal of Mn^{2+} does not change in the presence of the interferents compared with the blank signal in the absence of interferents. The interference study indicates that the proposed method can be applied for the determination of analytes in real samples with a complex matrix.

Sensitive Detection of Paraoxon. Paraoxon, an OP that could inhibit the catalytic activity of BChE, was detected by the present method. With more paraoxon in the sample, more effectively BChE is inhibited and less Mn^{2+} is generated. Thus, the ESR signal is inversely proportional to paraoxon's concentration and can be used to evaluate the level of paraoxon in the sample. The spectra are shown in Figure 4a. With the increase of paraoxon's concentration, the ESR signal first goes down linearly and then decreases slowly until reaching a platform close to zero. The standard curve of ESR signal vs paraoxon's concentration is constructed with [BChE] fixed at 20 U L^{-1} and displayed in Figure 4b. The linear part of the curve between 0 and 15 ng mL^{-1} is well fitted with the correlation coefficient r equal to 0.9993 (see the inset graph in Figure 4b). The regression equation is ESR signal = −0.4797 (±0.0069) [Paraoxon] + 8.12797 (±0.04778). The LOD of

https://doi.org/10.1021/acs.analchem.2c03708
Anal. Chem. 2022, 94, 16189−16195

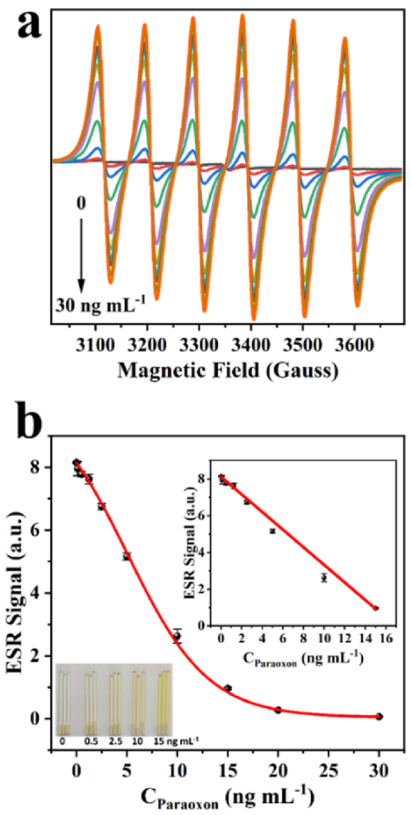

Figure 4. (a) ESR spectra for analytical samples with different concentrations of paraoxon (0, 0.1, 0.5, 1.25, 2.5, 5.0, 10, 15, 20, 30 ng mL^{-1}). (b) Plot of ESR signal vs paraoxon's concentration. Inset (right) displays the linear fit in the range of 0 to 15 ng mL^{-1}. Inset (left) shows the color change of analytical samples in capillary tubes (three analytical samples in capillary tubes for each concentration) with increasing paraoxon's concentration from 0 to 15 ng mL^{-1}. The error bar represents SD.

the method (3SD/slope with $n = 7$) for detecting paraoxon is estimated to be 0.076 ng mL^{-1}. The detection range is from 0.25 to 30 ng mL^{-1}.

In Table S2, the LOD and detection range of the present method for detecting an OP (paraoxon) are compared with those achieved by other methods from publications. The LOD of the present method (0.076 ng mL^{-1}) is low enough considering that the LODs in publications listed in Table S2 lie between 0.053 and 6.7 ng mL^{-1}. The detection range of the present method (0.25−30 ng mL^{-1}) spreads over more than 2 orders of magnitude. Such a wide detection range is also satisfactory compared with those reported in other works in Table S2, which are between 1 and 3 orders of magnitude.

Although the method has a good sensitivity with a low detection limit, the maximum detectable paraoxon concentration is 30 ng mL^{-1}, as it could cause problems for samples with a high OP level. In such a case, gradient dilution might be needed in sample pretreatment.

Inhibition of BChE by Other OPs. Nine other OPs, including dichlorvos, profenofos, isocarbophos, methyl paraoxon, malathion, malaoxon, parathion, chlorpyrifos, and chlorpyrifos oxon, were also detected by this method at a concentration of 15 ng mL^{-1}. The inhibited percentages of BChE's activity in the presence of the nine OPs and paraoxon are plotted in Figure 5. Of all the pesticides we tested, paraoxon and chlorpyrifos oxon were found to be highly toxic

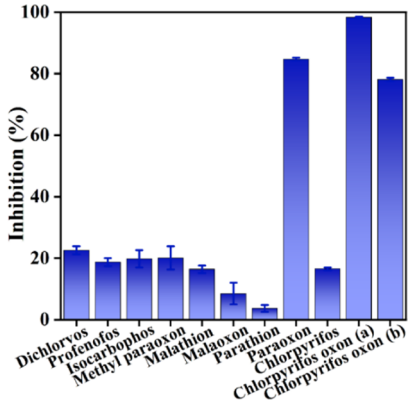

Figure 5. Inhibition of BChE's activity in the presence of dichlorvos, profenofos, isocarbophos, methyl paraoxon, malathion, malaoxon, parathion, paraoxon, chlorpyrifos, and chlorpyrifos oxon. The concentrations of dichlorvos, profenofos, isocarbophos, methyl paraoxon, malathion, malaoxon, parathion, paraoxon, and chlorpyrifos are all 15 ng mL^{-1}, respectively, corresponding to 67.9, 40.1, 51.9, 60.7, 45.4, 47.7, 51.5, 54.5, and 42.8 nmol L^{-1}. For chlorpyrifos oxon, two concentrations 15 (chlorpyrifos oxon (a)) and 0.125 (chlorpyrifos oxon (b)) ng mL^{-1} were used, corresponding to 44.8 and 0.37 nmol L^{-1}. The error bar represents SD.

to BChE (see Figure 5). For chlorpyrifos oxon, the inhibition percentage at 15 ng mL^{-1} was close to 100%, and when the concentration was 0.125 ng mL^{-1}, the inhibition percentage was still close to 80%.

All OP molecules have a phosphorus atom forming either a P═O bond or a P═S bond. OP with the P═O bond is an oxon pesticide and OP with the P═S bond is a thion pesticide.[26] Most thion pesticides such as parathion are converted to its oxon form paraoxon in the metabolic process and then become more toxic with higher anti-cholinesterase potency.[27] From our results, at the same concentration (15 ng mL^{-1}), two oxon pesticides (paraoxon and chlorpyrifos oxon) have much higher capability in inhibiting BChE compared to their thion forms parathion and chlorpyrifos. Based on the results, the poor inhibition ability of another two thion pesticides, including isocarbophos and malathion, can be explained.

On the other hand, paraoxon and chlorpyrifos oxon both have a diethyl phosphate moiety. Law et al. demonstrated using a series of dialkyl phenyl phosphates that the binding affinity between OP and BChE (from equine serum) increased as a function of alkyl chain length, with diethyl phosphate having a much lower inhibition constant than dimethyl phosphate.[28] This could explain the greater inhibition capability of paraoxon and chlorpyrifos oxon over the three dimethyl phosphate pesticides, including methyl paraoxon, dichlorvos, and malaoxon. Also, the low BChE inhibition by methyl paraoxon, dichlorvos, and malaoxon can be explained by spontaneous reactivation.[29,30] These inhibitors form dimethylphosphoryl adducts on BChE. Dimethylphosphoryl-inhibited BChE could spontaneously regain some activity during the incubation at 37 °C.[31] In contrast, for diethylphosphoryl-inhibited BChE (paraoxon and chlorpyrifos oxon), the rate of regain of activity is so slow and the measurement of inhibition would not be influenced.[29]

When inhibiting BChE from equine serum, the more toxicity of paraoxon relative to other pesticides has been found in previous publications.[3,5,32] For example, Tian et al. found that

https://doi.org/10.1021/acs.analchem.2c03708
Anal. Chem. 2022, 94, 16189−16195

when inhibiting equine BChE paraoxon had a much lower IC_{50} than dichlorvus and methyl paraoxon.[32] Chlorpyrifos oxon was found to be a very potent inhibitor to BChE from equine serum with a LOD as low as 0.008 nmol L^{-1}.[33] These results are consistent with ours.

Demonstration of No Interference from the Reaction of OP with BChE. We performed some experiments in order to further prove the reliability of the proposed ESR method and to prove that the ESR signal is from the reaction of substrate BTCh with BChE but not from the reducing agents released from the reaction of OP with BChE. The detailed results are displayed in the Supporting Information and Figures S4−S7.

Detection of Paraoxon in Chinese Cabbage. The accuracy of the present method was proved through the recovery experiment. The Chinese cabbage sample in the control group was spiked, respectively, with three concentrations (2.5, 5.0, and 10.0 ng mL^{-1}) of paraoxon. The extraction solution was first reacted with BChE (20 U L^{-1}) and BTCh and then reacted with MnO_2, and the resulting analytical samples were analyzed by ESR. The results is shown in Table 1, and the recoveries of paraoxon ranged from 96.5 and 102.8%.

Table 1. Detection of Spiked Paraoxon in the Extract of Chinese Cabbage Leaves

spiked (ng mL^{-1})	found (ng mL^{-1})	recovery (%)	RSD (n = 3, %)
2.50	2.57 ± 0.24	102.8	9.7
5.00	4.87 ± 0.64	97.4	12.7
10.00	9.65 ± 0.56	96.5	5.6

The method was also applied for the detection of paraoxon extracted from the planted Chinese cabbage after being sprayed with the standard solution of paraoxon. The image of planted Chinese cabbage and its extraction solution are shown in Figure S8. The concentration of the paraoxon residue found in the extract of sprayed Chinese cabbage is 326.7 ng mL^{-1}, which is consistent with the result 286.3 ng mL^{-1} obtained by HPLC. The satisfactory analytical results of the Chinese cabbage extract indicate that the present method is practical for detecting the residue of OPs in real plant samples.

For some food samples such as fruits containing high levels of ascorbic acid (i.e., vitamin C) which could reduce MnO_2 and interfere with the result, the sample should be pretreated either by a thermal treatment at 90 °C for 5 min to destroy the structure of ascorbic acid[34] or by using special chemical reagents when extracting OPs from the sample such as acetonitrile in which ascorbic acid is not soluble.[3] However, the reductive substances such as glutathione existing in blood or serum samples can decompose MnO_2 nanosheets, thus the present method may not be applicable to the detection of OPs in real blood or serum samples.

CONCLUSIONS

This work presents a novel ESR method for evaluation of BChE's activity and detection of OPs. The ESR signal is "turned on" when MnO_2 nanosheets with no ESR signal are decomposed and reduced to Mn^{2+} with a well-resolved six-line ESR spectrum. One advantage of the method is that there is no background signal when no BChE was added to the reaction system. Benefiting from the capability of ESR spectroscopy in the direct detection of Mn^{2+} in the presence of MnO_2, the method is label-free and much simpler compared with other methods in which usually an extra probe besides MnO_2 is necessary. The method is highly sensitive for the determination of BChE with a LOD of 0.042 U L^{-1} and paraoxon with a LOD of 0.076 ng mL^{-1}. With good accuracy and anti-interference ability, the present method is prospective in the sensitive detection of OPs in real plant samples. Such a simple, sensitive, and label-free strategy with zero background could be a promising platform for sensing enzymes catalyzing the generation of reductive substances and their inhibitors.

ASSOCIATED CONTENT

Supporting Information

The Supporting Information is available free of charge at https://pubs.acs.org/doi/10.1021/acs.analchem.2c03708.

Reagents and instruments; experimental procedures and schematic illustration of preparing MnO_2 nanosheets; optimization of assay conditions; demonstration of no interference from the reaction of OP with BChE; ESR signal in the presence of interfering substances; image of Chinese cabbage sprayed with paraoxon and image of the Chinese cabbage extraction solution after filtration; and comparison of analytical performance of the work with other publications for the determination of BChE's activity and OPs (PDF)

AUTHOR INFORMATION

Corresponding Author

Ziwei Zhang − *College of Chemistry, Jilin Province Research Center for Engineering and Technology of Spectral Analytical Instruments, Jilin University, Changchun 130012, PR China;* orcid.org/0000-0003-4834-4964; Phone: +86 13610709861; Email: zzw@jlu.edu.cn; Fax: +86 431 85112355

Authors

Li Tang − *College of Chemistry, Jilin Province Research Center for Engineering and Technology of Spectral Analytical Instruments, Jilin University, Changchun 130012, PR China*

Chunyu Wang − *State Key Laboratory of Supramolecular Structure and Materials, Jilin University, Changchun 130012, PR China*

Sizhu Tian − *College of Chemistry, Jilin Province Research Center for Engineering and Technology of Spectral Analytical Instruments, Jilin University, Changchun 130012, PR China*

Zhimin Zhang − *College of Chemistry, Jilin Province Research Center for Engineering and Technology of Spectral Analytical Instruments, Jilin University, Changchun 130012, PR China*

Yong Yu − *College of Instrumentation and Electrical Engineering, Jilin University, Changchun 130061, PR China*

Daqian Song − *College of Chemistry, Jilin Province Research Center for Engineering and Technology of Spectral Analytical Instruments, Jilin University, Changchun 130012, PR China;* orcid.org/0000-0002-4866-1292

Complete contact information is available at: https://pubs.acs.org/10.1021/acs.analchem.2c03708

Notes

The authors declare no competing financial interest.

https://doi.org/10.1021/acs.analchem.2c03708
Anal. Chem. 2022, 94, 16189−16195

REFERENCES

(1) Ma, J.; Ma, L.; Cao, L.; Miao, Y.; Dong, J.; Shi, Y. E.; Wang, Z. *Microchim. Acta* **2021**, *188*, 392.
(2) Guo, L.; Zhang, Y. J.; Yu, Y. L.; Wang, J. H. *Anal. Chem.* **2020**, *92*, 14806−14813.
(3) Yan, X.; Song, Y.; Zhu, C.; Li, H.; Du, D.; Su, X.; Lin, Y. *Anal. Chem.* **2018**, *90*, 2618−2624.
(4) Cai, Y.; Zhu, H.; Zhou, W.; Qiu, Z.; Chen, C.; Qileng, A.; Li, K.; Liu, Y. *Anal. Chem.* **2021**, *93*, 7275−7282.
(5) Wu, X.; Song, Y.; Yan, X.; Zhu, C.; Ma, Y.; Du, D.; Lin, Y. *Biosens. Bioelectron.* **2017**, *94*, 292−297.
(6) Sun, J.; Lynn, B. C. *J. Am. Soc. Mass Spectrom.* **2007**, *18*, 698−706.
(7) Cappiello, A.; Famiglini, G.; Palma, P.; Mangani, F. *Anal. Chem.* **2002**, *74*, 3547−3554.
(8) Notardonato, I.; Salimei, E.; Russo, M. V.; Avino, P. *Anal. Bioanal. Chem.* **2018**, *410*, 3285−3296.
(9) Russo, M. V.; Campanella, L.; Avino, P. *J. Chromatogr. B: Anal. Technol. Biomed. Life Sci.* **2002**, *780*, 431−441.
(10) Mammana, S. B.; Berton, P.; Camargo, A. B.; Lascalea, G. E.; Altamirano, J. C. *Electrophoresis* **2017**, *38*, 1334−1343.
(11) Wang, C.; Li, X.; Liu, Y.; Guo, Y.; Xie, R.; Gui, W.; Zhu, G. *J. Agric. Food Chem.* **2010**, *58*, 5658−5663.
(12) Huang, D.; Zhao, J.; Wang, M.; Zhu, S. *Food Control* **2020**, *108*, No. 106835.
(13) He, Y.; Hu, F.; Zhao, J.; Yang, G.; Zhang, Y.; Chen, S.; Yuan, R. *Anal. Chem.* **2021**, *93*, 8783−8790.
(14) Wang, K.; Wang, Y.; Li, Q.; Liu, Z.; Liu, S. *Sens. Actuators, B* **2022**, *351*, No. 130977.
(15) Sohal, N.; Maity, B.; Shetti, N. P.; Basu, S. *ACS Appl. Nano Mater.* **2021**, *4*, 2285−2302.
(16) Liu, X.; Zou, L.; Yang, X.; Wang, Q.; Zheng, Y.; Geng, X.; Liao, G.; Nie, W.; Wang, K. *Anal. Chem.* **2019**, *91*, 7943−7949.
(17) Gao, W.; Liu, Z.; Qi, L.; Lai, J.; Kitte, S. A.; Xu, G. *Anal. Chem.* **2016**, *88*, 7654−7659.
(18) Liu, H.; Wei, L.; Hua, J.; Chen, D.; Meng, H.; Li, Z.; Xiao, L. *Nanoscale* **2020**, *12*, 10390−10398.
(19) Zhang, Y.; Wei, Y.; Liu, P.; Zhang, X.; Xu, Z.; Tan, X.; Chen, M.; Wang, J. *Anal. Chem.* **2021**, *93*, 11540−11546.
(20) Davies, M. J. *Methods* **2016**, *109*, 21−30.
(21) Escudero, R.; Segura, J.; Velasco, R.; Valhondo, M.; Romero de Avila, M. D.; Garcia-Garcia, A. B.; Cambero, M. I. *Food Chem.* **2019**, *276*, 315−321.
(22) Xia, P.; Cheng, B.; Jiang, J.; Tang, H. *Appl. Surf. Sci.* **2019**, *487*, 335−342.
(23) Tian, S.; Li, X.; Jiang, J.; Tang, L.; Zhang, H.; Yu, Y.; Zhang, Z. *Sens. Actuators, B* **2021**, *338*, No. 129835.
(24) Cohn, M.; Townsend, J. *Nature* **1954**, *173*, 1090−1091.
(25) Carpenter, R. *Geochim. Cosmochim. Acta* **1983**, *47*, 875−885.
(26) Obare, S. O.; De, C.; Guo, W.; Haywood, T. L.; Samuels, T. A.; Adams, C. P.; Masika, N. O.; Murray, D. H.; Anderson, G. A.; Campbell, K.; Fletcher, K. *Sensors* **2010**, *10*, 7018−7043.
(27) Sparling, D. W.; Fellers, G. *Environ. Pollut.* **2007**, *147*, 535−539.
(28) Law, K. S.; Acey, R. A.; Smith, C. R.; Benton, D. A.; Soroushian, S.; Eckenrod, B.; Stedman, R.; Kantardjieff, K. A.; Nakayama, K. *Biochem. Biophys. Res. Commun.* **2007**, *355*, 371−378.
(29) Mason, H. J.; Waine, E.; Stevenson, A.; Wilson, H. K. *Hum. Exp. Toxicol.* **1993**, *12*, 497−503.
(30) Worek, F.; Diepold, C.; Eyer, P. *Arch. Toxicol.* **1999**, *73*, 7−14.
(31) Skrinjaric-spoljar, M.; Simeon, V.; Reiner, E. *Biochim. Biophys. Acta* **1973**, *315*, 363−369.
(32) Tian, J.; Chen, X.; Xie, Y.; Lu, Y.; Xu, W.; Xu, L.; Du, B. *J. Integr. Agric.* **2016**, *15*, 684−693.
(33) Sigolaeva, L. V.; Gladyr, S. Y.; Mergel, O.; Gelissen, A. P. H.; Noyong, M.; Simon, U.; Pergushov, D. V.; Kurochkin, I. N.; Plamper, F. A.; Richtering, W. *Anal. Chem.* **2017**, *89*, 6091−6098.
(34) Li, H.; Lv, W.; Yang, Q.; Li, Q.; Li, F. *J. Agric. Food Chem.* **2021**, *69*, 6087−6095.

https://doi.org/10.1021/acs.analchem.2c03708
Anal. Chem. 2022, 94, 16189−16195